

## Griseorhodins D–F, Neuroactive Intermediates and End Products of Post-PKS Tailoring Modification in Griseorhodin Biosynthesis

Zhenjian Lin,<sup>†</sup> Malcolm M. Zachariah,<sup>†</sup> Lenny Maret,<sup>†,§</sup> Ronald W. Hughen,<sup>§</sup> Russell W. Teichert,<sup>⊥</sup> Gisela P. Concepcion,<sup>‡</sup> Margo G. Haygood,<sup>||</sup> Baldomero M. Olivera,<sup>⊥</sup> Alan R. Light,<sup>§</sup> and Eric W. Schmidt<sup>\*,†,⊥</sup>

<sup>†</sup>Department of Medicinal Chemistry, L.S. Skaggs Pharmacy Institute, University of Utah, Salt Lake City, Utah 84112, United States

<sup>‡</sup>Marine Science Institute, University of the Philippines, Diliman, Quezon City 1101, Philippines

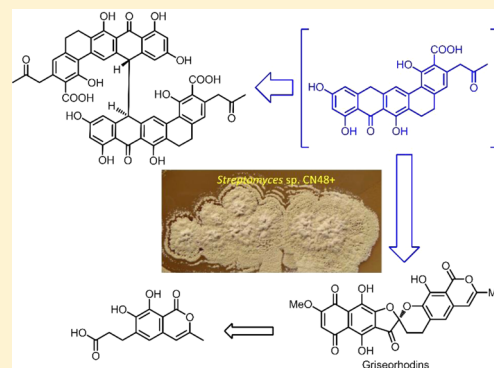
<sup>§</sup>Department of Anesthesiology, University of Utah, Salt Lake City, Utah 84112, United States

<sup>⊥</sup>Department of Biology, University of Utah, Salt Lake City, Utah 84112, United States

<sup>||</sup>Department of Environmental and Biomolecular Systems, OGI School of Science & Engineering, Oregon Health & Science University, Beaverton, Oregon 97006, United States

### Supporting Information

**ABSTRACT:** The griseorhodins belong to a family of extensively modified aromatic polyketides that exhibit activities such as inhibition of HIV reverse transcriptase and human telomerase. The vast structural diversity of this group of polyketides is largely introduced by enzymatic oxidations, which can significantly influence the bioactivity profile. Four new compounds, griseorhodins D–F, were isolated from a griseorhodin producer, *Streptomyces* sp. CN48+, based upon their enhancement of calcium uptake in a mouse dorsal root ganglion primary cell culture assay. Two of these compounds, griseorhodins D1 and D2, were shown to be identical to the major, previously uncharacterized products of a *grhM* mutant in an earlier griseorhodin biosynthesis study. Their structures enabled the establishment of a more complete hypothesis for the biosynthesis of griseorhodins and related compounds. The other two compounds, griseorhodins E and F, represent new products of post-polyketide synthase tailoring in griseorhodin biosynthesis and showed significant binding activity in a human dopamine active transporter assay.



Griseorhodins belong to a large family of bioactive, aromatic polyketides that are synthesized in actinomycetes by type II polyketide synthase (PKS) proteins.<sup>1,2</sup> The closest relatives of griseorhodin originate as pentangular polyketides that undergo reduction in the C-19/20 region (Figure 1A). Within this group (Figure 1), griseorhodins, fredericamycins, and benastatins have been extensively studied.<sup>3</sup> These compounds almost certainly originate in very similar polyketide products that are reduced in the C-19/20 region, but that differ in chain length because they originate with starter units of different lengths.<sup>1</sup> After the polyketide assembly and C-19/20 region reduction steps, the compounds are tailored by modifying enzymes, of which oxidases are especially prevalent. The major structural differences between the mature natural products are introduced during these tailoring steps.<sup>4</sup> For example, the early intermediates en route to griseorhodin undergo a series of steps culminating in oxidative C–C bond cleavage and rearrangement to yield the mature metabolites.<sup>5</sup> By contrast, benastatins undergo an early methylation event, and the final products contain the same core carbon skeleton as found in the post-PKS intermediate.<sup>6</sup> Fredericamycin undergoes a tailoring event leading to a carbocyclic moiety.<sup>7</sup> Finally,

these mature products undergo a further series of degradation reactions in the producing bacteria to yield a large number of known products.<sup>6,7</sup>

In the polyketide group that exhibits reduction in the C-19/20 region, the first post-PKS intermediate is thought to be an unstable monomer that readily undergoes radical reactions.<sup>5,7</sup> <sup>1</sup>H NMR spectra have been obtained for these intermediates in fredericamycin and griseorhodin biosynthesis, but the compounds have not been completely characterized.<sup>5,7</sup> In benastatin biosynthesis,<sup>6</sup> methyl groups are added at C-8 to this unstable intermediate, leading to the stable benastatin product. When the C-methyltransferase was knocked out, instead of obtaining a monomeric precursor, a mixture of unstable dimers was obtained, which readily broke down in the presence of air. These dimers were characterized by NMR, revealing the probable intermediate in benastatin biosynthesis (Figure 1B).<sup>6</sup>

Received: February 17, 2014

Published: May 1, 2014

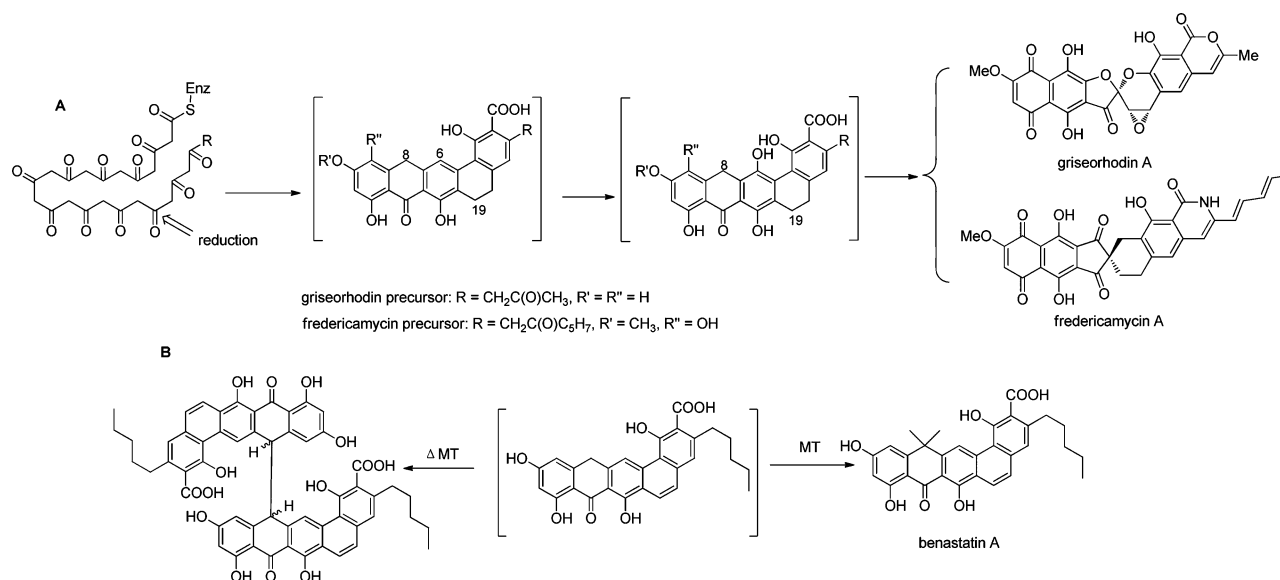
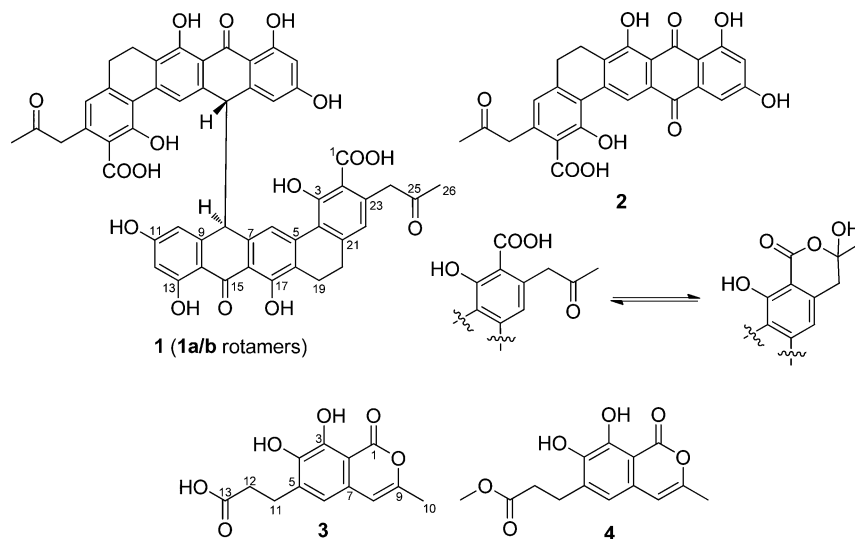


**Figure 1.** Structural diversity in the griseorhodin and its close biosynthetic relatives. (A) Postulated early steps in griseorhodin and fredericamycin biosynthesis. The structures of the intermediates in brackets are supported by <sup>1</sup>H NMR spectra and MS data. Here, we show that for the griseorhodin case the spectra represent those of a dimer. (B) Benastatin biosynthesis. A methyltransferase knockout led to accumulation of an unstable dimer, while methylation affords the natural product. The dimer in the griseorhodin pathway is similar to that of benastatin.

### Chart 1



We have been studying metabolites from bacterial associates of marine mollusks.<sup>8</sup> One of these strains, *Streptomyces* sp. CN48+, provided an extract that was bioactive in a neuroassay. The active components were identified as a series of novel compounds, which included both dimers of griseorhodin precursors and griseorhodin degradation products. The precursor dimers **1a** and **1b** were shown to be identical to the earliest known intermediate in griseorhodin biosynthesis, which was previously uncharacterized.<sup>5</sup> Like the early benastatin intermediate,<sup>6</sup> it exists as a series of unstable dimers, which may be the true substrates of early biosynthetic tailoring enzymes. These early precursor dimers and novel degradation products **3** and **4** provide information that aids in understanding the griseorhodin biosynthetic pathway.

### RESULTS AND DISCUSSION

Extracts of strain CN48+ were strongly active in the mouse dorsal root ganglion (DRG) assay, directly stimulating Ca<sup>2+</sup> influx. In an assay-guided procedure, the active extract was subjected to C<sub>18</sub> flash chromatography, followed by HPLC, to yield three neuroactive compounds, griseorhodins D–F (**1**, **3**, and **4**), which were responsible for the activity of the extract.

The molecular formula C<sub>52</sub>H<sub>38</sub>O<sub>16</sub> was assigned to each of the two constitutional isomers (**1a** and **1b**) on the basis of HRESIMS analysis. <sup>1</sup>H, <sup>13</sup>C, HSQC, HMBC, COSY, and NOESY NMR spectra were used in the structure determination. The <sup>1</sup>H NMR spectrum of **1a** showed signals of 17 protons, including three exchangeable hydroxyl protons, four singlet aromatic protons, a singlet methine proton, six methylene protons, and three methyl protons (Table 1). In CD<sub>3</sub>CN, the <sup>1</sup>H NMR spectrum of **1a** had several unusually broad peaks, which complicated the structural analysis. These

Table 1. NMR Data of Compound 1a and 1b in CD<sub>3</sub>CN-*d*<sub>3</sub>

no.	1a		1b	
	$\delta_C$	$\delta_H$ (J in Hz)	$\delta_C$	$\delta_H$ (J in Hz)
1	ND <sup>a</sup>		ND	
2	108.2 C		108.0 C	
3	161.1 C		ND	
4	120.7 C		121.1 C	
5	150.1 C		ND	
6	120.9 CH	7.42 brs	ND	7.28 brs
7	139.2 C			
8	57.7 CH	4.37 s	57.5 CH	4.46 s
9	145.4 C		ND	
10	109.7 CH	6.00 brs	109.2 CH	6.35 brs
11	164.2 CH		ND	
12	102.7 CH	6.22 s	102.6 CH	6.15 s
13	165.2 C		165.3 C	
14	111.3 C		112.4 C	
15	192.0 C		ND	
16	116.4 C		115.1 C	
17	158.1 C		158.6 C	
18	125.1 C		125.2 C	
19	20.2 CH <sub>2</sub>	2.76 m; 2.33 m	20.4 CH <sub>2</sub>	2.83 m; 2.50 m
20	31.2 CH <sub>2</sub>	2.74 m	30.7 CH <sub>2</sub>	2.73 m
21	ND		ND	
22	120.4 CH	6.75 s	120.2 CH	6.74 s
23	140.1 C		ND	
24	ND	3.27 brs	ND	3.23 brs
25	ND		ND	
26	28.5 CH <sub>3</sub>	1.76 s	28.2 CH <sub>3</sub>	1.75 s
17-OH		11.87 s		12.10 s
13-OH		11.94 s		11.80 brs
1-COOH		12.16 brs		12.3 brs

<sup>a</sup>ND: not detected.

broad signals were attributed to isomers that were interconverting on the NMR time-scale rather than to exchangeable protons. Two broad singlet proton signals at  $\delta_H$  6.00 and 7.42, which have no HSQC correlation, were assigned as aromatic methine protons because they could not be exchanged with extensive D<sub>2</sub>O treatment. Similarly, a broad signal for two protons at  $\delta_H$  3.27 with a 35 Hz peak width at half-height also was not exchangeable in D<sub>2</sub>O and showed a NOESY correlation with a methyl signal at  $\delta_H$  1.76, indicating that the signal corresponded to methylene protons.

We were able to observe the HMBC correlations (Figure 2) for every sharp proton signal (one methine proton, two aromatic singlet protons, two exchangeable phenol hydroxyl protons, and one methylene proton): from H-8 to six aromatic sp<sup>2</sup>-hybridized carbons (C-7,  $\delta_C$  139.2; C-9,  $\delta_C$  145.4; C-6,  $\delta_C$  120.9; C-16,  $\delta_C$  116.4; C-10,  $\delta_C$  109.7; C-14,  $\delta_C$  111.3), from H-10 to C-13, C-14, and C-10, from H-22 to C-20, C-4, and C-2, from 17-OH to C-17, C-18, and C-16, from 13-OH to C-13, C-14, and C-12, and from H-19 to C-5. Together with a COSY correlation between H-20 and H-19 and NOESY correlations between H-8/H-10 and H-8/H-6, these HMBC signals indicated a polyphenol substructure. Furthermore, the chemical shifts of the two phenol hydroxyl protons ( $\delta_H$  11.94 and 11.87) indicated the presence of a conjugated ketone, which was further confirmed by a quaternary carbon observed at 192.0 ppm in the <sup>13</sup>C NMR spectrum. Finally, an HMBC correlation

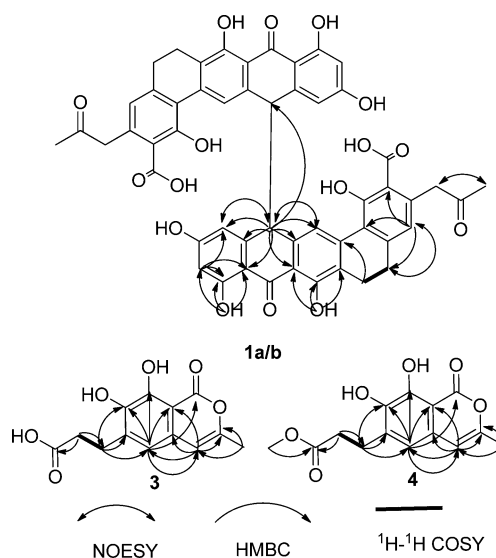


Figure 2. Key NOESY, HMBC, and COSY correlations for compounds 1a, 1b, 3, and 4.

between H-8 and C-8 in both 1a and 1b indicated that the compounds were dimeric and fused at C-8.

Chemical degradation experiments were sufficient to elucidate the remaining connectivities in 1a and 1b. Compounds 1a/b were not stable when exposed to air, especially in DMSO solutions. Both 1a and 1b were slowly converted to a red compound, 2, which could be purified by HPLC. NMR experiments showed that 2 was identical to the previously reported metabolite KS-619-1.<sup>9</sup> In fact, the only major difference of the NMR data between 1a/b and 2 was the presence of a methine residue ( $\delta_H$  4.37 and  $\delta_C$  57.7 for 1a;  $\delta_H$  4.46 and  $\delta_C$  57.5 for 1b) in place of a quinone carbonyl group. Therefore, the core structure of compounds 1a/b was determined. The core structure of 1a/b presented half the number of atoms in the molecular formula of 1a/b (C<sub>26</sub>H<sub>19</sub>O<sub>8</sub> vs C<sub>52</sub>H<sub>38</sub>O<sub>16</sub>), further reinforcing that 1a and 1b are homodimers.

Mass spectrometric data provided further evidence that 1a/b were dimers of the reduced form of 2 (Figure 3). In particular, the ion at *m/z* 458 suggested a radical ion fragment [M/2 - H]<sup>-</sup>. Another ion at *m/z* 414, which is equivalent to a loss of 44 Da in comparison to an ion at *m/z* 458, suggested loss of CO<sub>2</sub>, while an ion at *m/z* 372 was assigned as loss of CH<sub>2</sub>CO. The fragmentation pattern of 1a/b was identical to that of 2, but with a mass shift of 16 Da resulting from the additional oxygen.

In hydroxylactones such as benastatin F<sup>3</sup> and precursors of fredericamycin,<sup>7</sup> an arylacetone group readily undergoes tautomerization to form the hydroxylactone. In analogy, we proposed that the H-16 and H-18 might be broadened by tautomerism. Following the benastatin F precedent, we treated compound 2 with a drop of 28% ammonium hydroxide, revealing the presence of the “missing” methylene and methyl protons and confirming the identity of the side chain. Unfortunately, ammonium hydroxide led to immediate decomposition of 1a/b.

1a/b are similar to products obtained in mutants of the benastatin pathway,<sup>6</sup> with the differences being the length and oxidation state of the side chain at C-3 and the saturation state of the C5–C6 bond. As found with the benastatin derivatives, NMR experiments were not sufficient to differentiate between possible stereoisomers at C8–C8'. This problem was

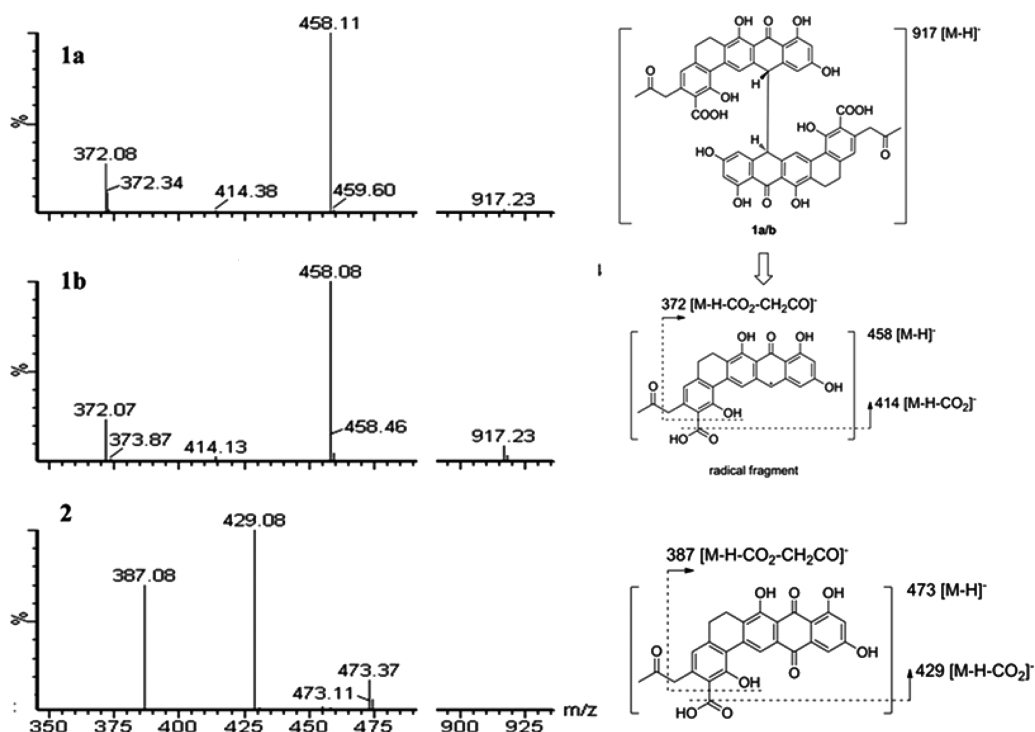


Figure 3. ESI-MS fragmentation of compounds 1a/b and 2.

previously solved in the benastatin case using molecular modeling,<sup>6</sup> which showed that one compound was a *meso* (*R,S*) dimer, existing as readily HPLC-separable rotamers. However, those rotamers interconverted over time. A second compound was racemic (*R,R*, *S,S*, or a combination of both) and existed as a single rotamer, which closely coeluted with one of the *meso* rotamers. The chemical shift differences between these proposed isomers were minor, and none exhibited different chemical shifts across the dimer interface. Here, the two isolated compounds were well separated by HPLC, and they slowly interconverted in the NMR tube. This interconversion was slower than for the benastatin relatives and was co-incident with monomer (**2**) formation. Nonetheless, this similarity makes it likely that **1a/1b** represent the *meso* (*R,S*) dimer. A third constitutional isomer closely coeluted with **1b**, but was present in minor amounts and could not be isolated. On the basis of similarity to the benastatin case, this may represent the *rac* isomer.

Griseorhodin E (**3**) was assigned a molecular formula of  $C_{13}H_{12}O_6$  on the basis of ESIMS analysis and 1D NMR data (Table 2). The  $^1H$  NMR spectrum of **3** showed the presence of two singlet aromatic protons at  $\delta_H$  6.89 and 6.45, two methylene groups at  $\delta_H$  3.07 and 2.17, and a methyl group at  $\delta_H$  2.28. The  $^{13}C$  NMR spectrum of **3** showed the presence of 13 signals, including two carbonyls, eight  $sp^2$  carbons, and three  $sp^3$  carbons. The ratio of proton number to carbon number suggested a highly substituted aromatic structure in **3**. The HMBC correlations from H-11 to C-4, C-5, C-6 and from H-6 to C-2, C-3, C-4 suggested a pentasubstituted phenyl ring. The chemical shifts of C-2 and C-3 indicated a 2,3-dihydroxy substitution. The  $^1H$ - $^1H$  COSY correlation between H-11 and H-12, along with the HMBC correlation from H-12 to the carbonyl carbon (C-13), suggested the presence of a 2-carboxyethyl group at C-5. The HMBC correlations from H-10 to C-9, C-8 and from H-8 to C-6, C-7, C-9, along with a long-

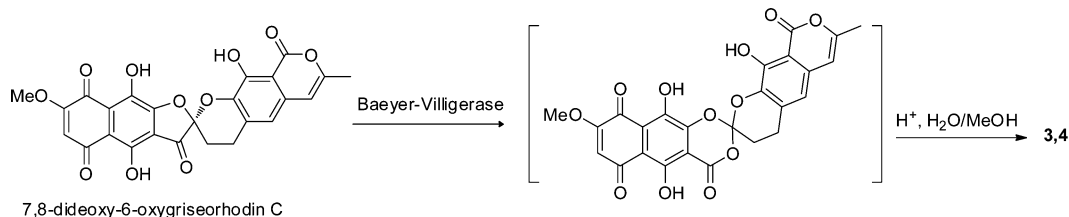
Table 2.  $^1H$  and  $^{13}C$  NMR Data of Compounds **3** and **4** in  $CD_3CN-d_3$

no.	3		4	
	$\delta_C$	$\delta_H$ (J in Hz)	$\delta_C$	$\delta_H$ (J in Hz)
1	167.6 C		167.6 C	
2	104.8 C		104.8 C	
3	148.8 C		148.9 C	
4	142.8 C		142.2 C	
5	137.9 C		137.6 C	
6	116.7 CH	6.89 s	117.5 CH	6.87 s
7	129.9 C		129.9 C	
8	104.6 CH	6.45 s	104.9 CH	6.45 s
9	152.4 C		152.2 C	
10	19.1 CH <sub>3</sub>	2.28 s	19.9 CH <sub>3</sub>	2.27 s
11	26.8 CH <sub>2</sub>	3.07 t (7.6)	28.8 CH <sub>2</sub>	3.05 t (7.6)
12	33.2 CH <sub>2</sub>	2.71 t (7.6)	33.8 CH <sub>2</sub>	2.72 t (7.6)
13	173.9 C		173.1 C	
13-OMe			52.4 CH <sub>3</sub>	3.66 s

distance correlation from H-6 to C-1, suggested a benzoenol lactone substructure in **3**. Together, these data were consistent with the structure assigned to **3**. The NMR spectra (Table 2) of griseorhodin F (**4**) were very similar to those of **3**. The only difference was an extra methoxyl group observed in the NMR spectra of **4**. The HMBC spectrum showed the proton of the methoxyl had a correlation to the carbonyl carbon C-1, indicating **4** is a methyl ester of **3**.

The precursor of **1a/b** is similar to a precursor in the benastatin pathway, which was proposed to be short-lived and to break down via reactive benzyl radicals.<sup>6</sup> By analogy, it seemed possible that **1a/b** were dimerized precursors in the griseorhodin pathway. Indeed, griseorhodins were also obtained from the culture broth of strain CN48+. To test this hypothesis, we sequenced the genome of CN48+. The resulting draft genome (11.5 Mbp) was assembled into 169 contigs (NS0 =

Scheme 1. Proposed Pathway for the Biosynthesis of 3 and 4



642 kbp). BLAST searching for aromatic type II polyketide synthase homologues in the genome revealed only a single significant hit (GenBank accession number KJ610894), which was nearly identical to the previously reported griseorhodin biosynthetic gene cluster<sup>2</sup> (GenBank accession number AF509565; identical gene content, syntenic, and 99% DNA sequence identical). Thus, genomic data strongly implicated the griseorhodin biosynthetic gene cluster as being responsible for griseorhodin D–F biosynthesis, since no other potential type II pathway was present in the genome.

Yunt et al.<sup>5a</sup> previously knocked out the genes potentially responsible for griseorhodin biosynthesis in *Streptomyces* sp. JP95, which like CN48+ was isolated from a marine invertebrate. When the gene *grhM* was deleted, two constitutional isomer intermediates with a measured molecular formula of  $C_{26}H_{20}O_8$  ( $m/z$  461.1240, nearly half of the molecular weight of **1a/b**) were obtained, while all downstream griseorhodin metabolites were abolished. Like **1a/b**, the products of the *grhM* mutant were unstable and difficult to work with. Initially, the *grhM* mutant products were postulated to be identical to the monomeric form of **1a/b**. However, in our examination of **1a/b**, the identical ion ( $m/z$  461.1) was also found in many mass spectrometry conditions, which was assigned as the major fragment of **1a/b**. Furthermore, examination of the HPLC data from Yunt et al.<sup>5b</sup> showed that the two major isomer products of *grhM* mutant had a very similar elution profile to **1a/b**. Their <sup>1</sup>H NMR spectra were almost identical to a spectrum of **1a/b**. Therefore, it seemed likely that deletion of *grhM* leads to accumulation of **1a/b**. To test this hypothesis, we extracted the compounds from the *grhM* mutant, which was kindly provided by Dr. Jörn Piel. Both HPLC-ESIMS and NMR experiments confirmed these compounds are identical. Therefore, **1a/1b** are the major products from the *grhM* mutant.

GrhM is similar to FdmM from fredericamycin biosynthesis.<sup>7</sup> FdmM was proposed to be an oxidase that performs the first post-PKS aromatic hydroxylation in the pathway.<sup>10</sup> Similar proteins are encoded in many different type II PKS pathways, where they may perform very similar functions.<sup>11</sup> In the griseorhodin pathway, GrhM appears to oxidize the C-14 position in **1a/b**. Subsequently, other positions in the polyketide are oxidized and modified by a series of tailoring enzymes, leading ultimately to formation of mature griseorhodins. Several other early intermediates in the pathway could also not be readily characterized.<sup>5</sup> We speculate that some of these compounds might also be dimeric forms. For example, the *grhM* mutant product was initially identified as possibly being the monomer by MS, but our analysis shows that the dimeric form readily provides ions corresponding to the monomer due to fragmentation. Under many conditions, this ion dominates the spectrum. This might also be true of some of the other intermediates in the series,<sup>7</sup> possibly indicating that

the dimeric forms could be the actual *in vivo* substrates of the early tailoring enzymes.

Oxidative metabolism might also lead to formation of **3** and **4**, which we propose to be breakdown products of griseorhodins. In this model, the spiroketal moiety of griseorhodins would be subject to further enzymatic carbon–carbon bond cleavage events, leading to formation of the degradation products (Scheme 1). It is noteworthy that compounds **1**, **3**, and **4** are major products of strain CN48+ under many different culture conditions, where they are produced in nearly the equivalent amounts to griseorhodins themselves. By contrast, it appears that these compounds are not major constituents of previously reported griseorhodin producers.<sup>5</sup> It is unclear what causes these differences, but here the availability of an additional strain led to the isolation and structure elucidation of abundant intermediates that might otherwise be difficult to obtain. For example, in the case of fredericamycin oxidation, isolation of early products required genetic manipulation.<sup>7</sup>

It seemed possible that the different product ratios in strain CN48+ might be due to differences in oxygen tension or oxidation state in the medium. Therefore, we manipulated the culture conditions either by adding  $H_2O_2$  or by limiting  $O_2$ . While peroxide increased the production of every compound, oxygen limitation decreased production of all compounds. Therefore, oxidation did not directly impact the production of dimers versus mature griseorhodin A formation. In different media conditions, CN48+ produced mainly the dimers **1a/b** when extra sodium was left out of the medium. When supplemented with NaCl, mainly mature griseorhodins A and **7**<sup>5</sup> were produced (Figure S8). It is well known that marine and other bacterial strains are salt responsive in terms of their chemical profiles.<sup>12</sup>

Compounds **1**, **3**, and **4** were identified because of their activity in the DRG assay. This phenotypic assay uses a primary culture of DRG neurons, which contains >12 individual cell types that respond differently to neuroactive agents.<sup>13–15</sup> The different responses are caused largely by different combinations of receptor and ion channel subtypes in these different cell types, which reflect their phenotype in nature. DRG neurons are the primary sensory neurons, and their individual functions reflect sensations such as touch, pain, heat, cold, and itch. Therefore, in a single assay, multiple, physiologically relevant phenotypes are simultaneously assayed. The assay is performed using a  $Ca^{2+}$ -responsive dye, Fura-2. In the DRG assay, **3** and **4** increased the  $Ca^{2+}$  concentration in over 80% of the DRG cells at 20  $\mu g/mL$ . By contrast, **1a** and **1b** did not directly depolarize cells, but instead potentiated the response to KCl. When **1a** and **1b** were administered at 10  $\mu g/mL$ , subsequent addition of 25 mM KCl led to an increase in the  $Ca^{2+}$  influx in comparison to controls in the same well.

To determine the potential molecular targets and potencies underlying these observed phenotypes, we further screened **1**–

4 at the National Institute of Mental Health's Psychoactive Drug Screening Program (PDSP). A primary assay was performed binding 46 targets at a final concentration of 10  $\mu\text{M}$  of each compound. Initial hits were obtained in radioligand displacement assays. For targets where significant binding activity was detected, secondary binding assays were performed, and  $K_i$  values were calculated using radioligand displacement with test compound concentrations from 1 to 10 000 nM. Only compound 3 exhibited activity below the 10  $\mu\text{M}$  threshold, and only in a human dopamine active transporter (DAT) assay, with a  $K_i$  of 557 nM. Compound 4 did not show any binding activity below 10  $\mu\text{M}$ . We could not find any report of DAT in DRG cells, making it unlikely that this target was responsible for the activity in the phenotypic assay.

## EXPERIMENTAL SECTION

**General Experimental Procedures.** UV spectra were obtained using a PerkinElmer Lambda2 UV/vis spectrometer. NMR data were collected using either a Varian INOVA 500 ( $^1\text{H}$  500 MHz,  $^{13}\text{C}$  125 MHz) NMR spectrometer with a 3 mm Nalorac MDBG probe or a Varian INOVA 600 ( $^1\text{H}$  600 MHz,  $^{13}\text{C}$  150 MHz) NMR spectrometer equipped with a 5 mm  $^1\text{H}$ [ $^{13}\text{C}$ , $^{15}\text{N}$ ] triple resonance cold probe with a z-axis gradient, utilizing residual solvent signals for referencing. High-resolution mass spectra (HRMS) were obtained using a Bruker (Billerica, MA, USA) APEXII FTICR mass spectrometer equipped with an actively shielded 9.4 T superconducting magnet (Magnex Scientific Ltd., UK), an external Bruker APOLLO ESI source, and a Synrad 50W  $\text{CO}_2$  CW laser.

**Bacterial Material.** *Streptomyces* sp. CN48+ was cultivated from *Chicoreus nobilis*, obtained by professional collectors near Mactan Island, Cebu, Philippines, as previously described.<sup>8</sup> The strain was cultured from dissected venom duct tissue and purified, and later the strain was recovered from a glycerol stock and used for further chemical analysis. The 16S gene was cloned using primers 8–27f (5'-AGAGTTTGATCCTGGCTCAG-3') and 1492r (5'-TACGGYTACCTGTACGACTT-3') and submitted to GenBank (accession number KJ400005).

**Fermentation and Extraction.** For the first-stage seed, an agar-grown culture of *Streptomyces* sp. CN48+ was inoculated into 150 mL of ISP2 medium (0.4% yeast extract, 1% malt extract, 0.4% glucose). After 3 days' incubation at 22 °C with shaking, the first stage (100 mL) was used to inoculate in a New Brunswick BioFlo110 fermenter containing 10 L of the medium ISP2, with or without addition of 2% NaCl, at 30 °C. After 8 days, the broth was centrifuged and the supernatant was extracted with Diaion HP-20 resin for 4 h. The resin was filtered through cheesecloth and washed with  $\text{H}_2\text{O}$  to remove salts. The filtered resin was eluted with MeOH to yield a primary extract. The MeOH eluate was dried under rotavap, and the water remaining was portioned three times against EtOAc. The organic layer was dried to yield the crude extract.

**Purification.** The extract from 2% NaCl ISP2 media culture was separated into six fractions (Fr1–Fr6) on a  $\text{C}_{18}$  column using step-gradient elution of MeOH in  $\text{H}_2\text{O}$  (40%, 50%, 60%, 70%, 80%, 100%). Fr3, eluting in 60% MeOH, was further purified by  $\text{C}_{18}$  HPLC using 50% MeOH in  $\text{H}_2\text{O}$  with 0.05% TFA to obtain compounds 3 (1.3 mg) and 4 (4.0 mg). The extract from NaCl-free media culture was separated into three fractions (Fr'1–Fr'3). Fr'3, eluting in 100% MeOH, was further purified by  $\text{C}_{18}$  HPLC using 87% MeCN in  $\text{H}_2\text{O}$  with 0.05% TFA to obtain compounds 1a (4.1 mg) and 1b (3.2 mg).

**Griseorhodin D1 (1a):** yellow solid; UV (MeOH)  $\lambda_{\text{max}}$  228, 303, 380 nm;  $^1\text{H}$  and  $^{13}\text{C}$  NMR (see Table 1); HRESIMS  $m/z$  919.2241 [ $\text{M} + \text{H}$ ]<sup>+</sup> (calcd for  $\text{C}_{52}\text{H}_{39}\text{O}_{16}$ , 919.2238).

**Griseorhodin D2 (1b):** yellow solid; UV (MeOH)  $\lambda_{\text{max}}$  228, 303, 380 nm;  $^1\text{H}$  and  $^{13}\text{C}$  NMR (see Table 1); HRESIMS  $m/z$  919.2255 [ $\text{M} + \text{H}$ ]<sup>+</sup> (calcd for  $\text{C}_{52}\text{H}_{39}\text{O}_{16}$ , 919.2238).

**Griseorhodin E (3):** pale yellow solid; UV (MeOH)  $\lambda_{\text{max}}$  233, 260, 362 nm;  $^1\text{H}$  and  $^{13}\text{C}$  NMR (see Table 2); ESIMS  $m/z$  279.1 [ $\text{M} + \text{H}$ ]<sup>+</sup>.

**Griseorhodin F (4):** pale yellow solid; UV (MeOH)  $\lambda_{\text{max}}$  233, 260, 362 nm;  $^1\text{H}$  and  $^{13}\text{C}$  NMR (see Table 2); ESIMS  $m/z$  265.1 [ $\text{M} + \text{H}$ ]<sup>+</sup>.

**Chemical Modification of Griseorhodin D.** Compound 2 was synthesized by dissolving 1a (2 mg) in  $\text{DMSO}-d_6$  (500  $\mu\text{L}$ ) and incubating the mixture for 10 days at  $-20$  °C. Compound 2 (55% yield) was purified by HPLC using 65% MeCN in  $\text{H}_2\text{O}$  with 0.05% TFA.

**DRG Assay.** DRG cells were obtained from mice, plated in medium with additives, and loaded with Fura-2 AM (Molecular Probes).<sup>13</sup> Experiments were performed as previously described.<sup>8e</sup>

**Receptor Affinity Screen.** Assays for the following receptors were performed by the PDSP/NIMH: (1) muscarinic receptors: M1, M2, M3, M4, M5; (2) serotonin receptors: 5ht1a, 5ht1b, 5ht1d, 5ht1e, 5ht2a, 5ht2b, 5ht2c, 5ht3, 5ht4, 5ht5a, 5ht6, 5ht7; (3) GABA receptors: BZP (rat brain site), GABA A, GABA B; (4) histaminergic receptors: H1, H2, H3, H4; (5) dopamine receptors: D1, D2, D3, D4, D5; (6) transporters: NET, SERT, DAT; (7) opiate receptors: DOR, KOR, MOR; (8) adrenergic receptors: Alpha1A, Alpha1B, Alpha1D, Alpha2A, Alpha2B, Alpha2C, Beta1, Beta2, Beta3; (9) others: Sigma 1, Sigma 2,  $\text{Ca}^+$  channel. Detailed online protocols are available for all assays at the PDSP/NIMH Web site (<http://pdsp.med.unc.edu/>).

## ASSOCIATED CONTENT

### Supporting Information

This material is available free of charge via the Internet at <http://pubs.acs.org>.

## AUTHOR INFORMATION

### Corresponding Author

\*Tel: 801-585-5234. Fax: 801-581-7087. E-mail: [ews1@utah.edu](mailto:ews1@utah.edu).

### Notes

The authors declare no competing financial interest.

## ACKNOWLEDGMENTS

This work was funded by ICBG grant U01TW008163 from Fogarty (NIH). We thank the government of the Philippines and the community of Mactan Island for permission to conduct this study. Binding assay data were generously provided by the National Institute of Mental Health's Psychoactive Drug Screening Program, contract no. HHSN-271-2008-00025-C (NIMH PDSP). The NIMH PDSP is directed by B. L. Roth MD, PhD, at the University of North Carolina at Chapel Hill and Project Officer J. Driscoll at NIMH, Bethesda, MD, USA.

## REFERENCES

- (1) Lackner, G.; Schenk, A.; Xu, Z.; Reinhardt, K.; Yunt, Z. S.; Piel, J.; Hertweck, C. *J. Am. Chem. Soc.* **2007**, *129*, 9306–9312.
- (2) Li, A.; Piel, J. *Chem. Biol.* **2002**, *9*, 1017–1026.
- (3) Xu, Z.; Schenk, A.; Hertweck, C. *J. Am. Chem. Soc.* **2007**, *129*, 6022–6030.
- (4) (a) Rix, U.; Fischer, C.; Remsing, L. L.; Rohr, J. *Nat. Prod. Rep.* **2002**, *19*, 542–580. (b) Hertweck, C.; Luzhetskyy, A.; Rebets, Y.; Bechthold, A. *Nat. Prod. Rep.* **2007**, *24*, 162–190.
- (5) (a) Yunt, Z.; Reinhardt, K.; Li, A.; Engeser, M.; Dahse, H.; Guetschow, M.; Bruhn, T.; Bringmann, G.; Piel, J. *J. Am. Chem. Soc.* **2009**, *131*, 2297–2305. (b) Yunt, Z. Chemical Investigation of *Streptomyces albus* Heterologous Expression Strains and the Biosynthesis of the Aromatic Polyketide Griseorhodin A. Ph.D. Thesis, University of Bonn, Bonn, Germany, 2012; p 272.
- (6) Schenk, A.; Xu, Z.; Pfeiffer, C.; Steinbeck, C.; Hertweck, C. *Angew. Chem., Int. Ed.* **2007**, *46*, 7035–7038.
- (7) Chen, Y.; Wendt-Pienkoski, E.; Rajski, S. R.; Shen, B. *J. Biol. Chem.* **2009**, *284*, 24735–24743.

- (8) (a) Lin, Z.; Antemano, R. R.; Hughen, R. W.; Tianero, M. D.; Peraud, O.; Haygood, M. G.; Concepcion, G. P.; Olivera, B. M.; Light, A.; Schmidt, E. W. *J. Nat. Prod.* **2010**, *73*, 1922–1926. (b) Lin, Z.; Reilly, C. A.; Antemano, R.; Hughen, R. W.; Marett, L.; Concepcion, G. P.; Haygood, M. G.; Olivera, B. M.; Light, A.; Schmidt, E. W. *J. Med. Chem.* **2011**, *54*, 3746–3755. (c) Lin, Z.; Flores, M.; Forteza, L.; Henriksen, N. M.; Concepcion, G. P.; Rosenber, G.; Haygood, M. G.; Olivera, B. M.; Light, A. R.; Cheatham, T. E.; Schmidt, E. W. *J. Nat. Prod.* **2012**, *75*, 644–649. (d) Lin, Z.; Torres, J. P.; Ammon, M. A.; Marett, L.; Teichert, R. W.; Reilly, C. A.; Kwan, J. C.; Hughen, R. W.; Flores, M.; Tianero, M. D.; Peraud, O.; Cox, J. E.; Light, A. R.; Villaraza, A. J.; Haygood, M. G.; Concepcion, G. P.; Olivera, B. M.; Schmidt, E. W. *Chem. Biol.* **2013**, *20*, 73–81. (e) Lin, Z.; Marett, L.; Hughen, R. W.; Flores, M.; Forteza, L.; Ammon, M. A.; Concepcion, G. P.; Espino, S.; Olivera, B. M.; Rosenberg, G.; Haygood, M. G.; Light, A. R.; Schmidt, E. W. *Bioorg. Med. Chem. Lett.* **2013**, *23*, 4867–4869. (f) Lin, Z.; Koch, M.; Pond, C. D.; Mabeza, G.; Seronay, R. A.; Concepcion, G. P.; Barrows, L. R.; Olivera, B. M.; Schmidt, E. W. *J. Antibiot.* **2014**, *67*, 121–126.
- (9) Yasuzawa, T.; Yoshida, M.; Shirahata, K.; Sano, H. *J. Antibiot.* **1987**, *40*, 1111–1114.
- (10) Wendt-Pienkowski, E.; Huang, Y.; Zhang, J.; Li, B.; Jiang, H.; Kwon, H.; Hutchinson, C. R.; Shen, B. *J. Am. Chem. Soc.* **2005**, *127*, 16442–16452.
- (11) Martin, R.; Sterner, O.; Alvarez, M. A.; De Clercq, E.; Bailey, J. E.; Minas, W. *J. Antibiot.* **2001**, *54*, 239–249.
- (12) Bugni, T. S.; Ireland, C. M. *Nat. Prod. Rep.* **2004**, *21*, 143–163.
- (13) Light, A. R.; Hughen, R. W.; Zhang, J.; Rainier, J.; Liu, Z.; Lee, J. *J. Neurophysiol.* **2008**, *100*, 1184–1201.
- (14) Teichert, R. W.; Raghuraman, S.; Memon, T.; Cox, J. L.; Foulkes, T.; Rivier, J. E.; Olivera, B. M. *Proc. Natl. Acad. Sci. U.S.A.* **2012**, *109*, 12758–12763.
- (15) Teichert, R. W.; Smith, N. J.; Raghuraman, S.; Yoshikami, D.; Light, A. R.; Olivera, B. M. *Proc. Natl. Acad. Sci. U.S.A.* **2012**, *109*, 1388–1395.